Dielectric Properties of Exfoliated Graphite Reinforced Flouroelastomer Composites

Deng Xu,[1] V. Sridhar,[1] S. P. Mahapatra,[1,2] Jin Kuk Kim[1]

[1]*Elastomer laboratory, Department of Polymer Science & Technology, Gyeongsang National University, Jinju, 660-701, South Korea*
[2]*Microcellular Plastics Manufacturing Laboratory, Department of Mechanical and Industrial Engineering, University of Toronto, Canada*

Received 14 May 2007; accepted 8 January 2008
DOI 10.1002/app.29183
Published online 30 October 2008 in Wiley InterScience (www.interscience.wiley.com).

ABSTRACT: Dielectric relaxation behavior of nano graphite reinforced flouroelastomer composites has been studied as a function of variation in filler in the frequency range of 0.01–10^5 Hz. The effect of variation in filler loadings on the complex and real parts of impedance was distinctly visible which has been explained on the basis of interfacial polarization of fillers in a heterogeneous medium and relaxation dynamics of polymer chains in the vicinity of fillers. The electric modulus formalism has been utilized to further investigate the conductivity and relaxation phenomenon. The frequency dependence of AC conductivity has been investigated by using Percolation theory. The phenomenon of percolation in the composites has been discussed based on the measured changes in electric conductivity and morphology of composites at different concentrations of the filler. The percolation threshold as studied by DC conductivity occurred in the vicinity of 2.5–3.5 phr of filler loading. Scanning electron microscope microphotographs showed agglomeration of the filler above this concentration and formation of a continuous network structure. © 2008 Wiley Periodicals, Inc. J Appl Polym Sci 111: 1358–1368, 2009

Key words: exfolaited graphite; flouroelastomers; nano composites; dielectric relaxation and percolation

INTRODUCTION

Many materials used in our daily life are composites, which often are made up of at least two constituents or phases. The outstanding mechanical properties of many composites, and especially the unique combination of low density with high strength and stiffness, have led not only to extensive research but also to highly developed technologies.[1,2]

Conductive polymer composites have received considerable attention due to their technological importance in a wide variety of applications such as electrostatic charge dissipation material in pressure sensitive sensors, transducers, EMI shielding material and as packaging material in electronics, aircraft and telecommunications. They are also used as antistatic materials in low temperature heaters, in energy storage devices such as batteries, fuel cells, and super capacitors and in hybrid power sources. Normally, the conductivity in a polymer is imparted by incorporation of electrically conductive fillers into the polymer matrix. Metal fillers,[3] carbon fibers[4] and conductive carbon black[5] have been used in practice.

Carbon blacks and silica have been traditionally used as reinforcing materials in elastomers. But recently much attention is being focused on the applicability of novel carbon based fillers like carbon silica dual phase filler,[6] carbon nano tubes[7] and nano graphite.[8] Graphite is composed of layered nanosheets with good electrical conductivity of 10^4 S/cm at room temperature. Normally in graphite, three sp^2 hybrid orbitals (each containing one electron) are formed from the 2s and two of the 2p orbitals of each carbon atom and participate in covalent bonding with three surrounding carbon atoms in the graphite planes. The fourth electron is located in the remaining 2p orbital, which projects above and below the graphite plane, to form part of a polyaromatic π-system. Delocalization of electrons in π-electron system is the cause of high stability and electrical conductivity.

The present study deals with the dielectric relaxation spectra of nano graphite reinforced flouroelastomers in the frequency range of 0.01–10^5 Hz as function of filler loading. The effect of variation in filler loading on dielectric characteristics like dissipation factor (loss tangent), real and complex parts of impedance, dielectric permittivity, and conductivity have been studied. Additionally the data obtained was also analyzed by electric modulus formalism.

EXPERIMENTAL

Materials

Flouroelastomer with 71% fluorine content was procured from Daikin, Japan under the trade name G-

Correspondence to: J. K. Kim (rubber@gnu.ac.kr).

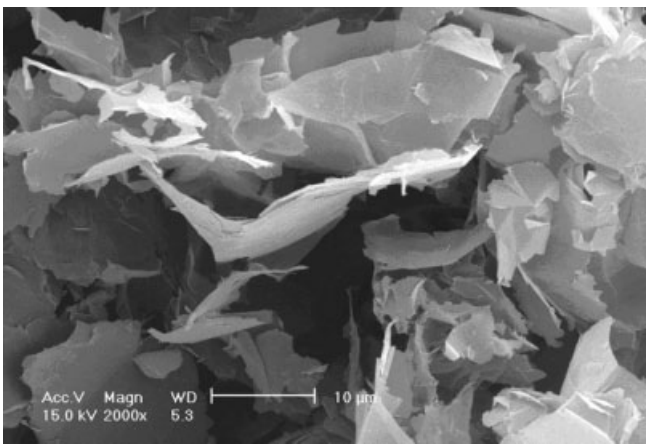

Figure 1 Representative SEM microphotograph of exfoliated graphite sheets produced by acid intercalation method.

902. The exfoliated graphite (xGnP-15) synthesized by acid intercalation method has been kindly supplied by Drzal group of Michigan State University.[9,10] Representative scanning electron microscope (SEM) microphotograph of the exfoliated nano graphite is shown in Figure 1. A peroxide curing system has been used in this study and the curatives are Trigonox 101 (2,5-dimethyl -2,5-bis (T-butylperoxy) hexane) in conjunctin with the coagent TAIC (Tri-Alyll IsoCyanurate).

Sample preparation

The compounds were mixed in a laboratory size (225 × 100 mm) mixing mill at a friction ratio of 1 : 1.25 according to ASTM D 3182 standards while carefully controlling the temperature, nip gap, mixing time, and uniform cutting operation. The temperature range for mixing was maintained at 80°C by carefully circulating water. After mixing, the elastomer compositions were molded in an electrically heated hydraulic press to optimum cure (90% of the maximum cure) using molding conditions determined by a Monsanto rheometer.

Testing

Dielectric relaxation spectra

Dielectric relaxation spectra of the vulcanizates were obtained by a Hioki 3522-50 HiTester LCR meter in the frequency range of 0.01–10^5 Hz using aluminum foil as blocking electrodes. AC conductivity (σ_{AC}) has been evaluated from dielectric data in accordance with the relation:

$$\sigma_{AC} = \omega\varepsilon_0\varepsilon' \tan\partial \quad (1)$$

where ω is $2\pi f$ (f is frequency), ε_0 is permittivity of the vacuum and dielectric constant or relative permittivity $\varepsilon' = C_p/C_0$ where C_p is the observed capacitance of the sample and C_0 is vacuum capacitance of the cell and is calculated using the expression $\varepsilon_0 A/d$ (where A is area of the sample and d is thickness of the sample) and $\tan\partial$ is the dielectric loss tangent.

Scanning electron microscopy

Morphology of the compounds has been studied using a SEM (Philips XL30 S FEG (Netherlands)), after auto sputter coating of the sample surface with gold.

RESULTS AND DISCUSSION

Phase angle

Figure 2 shows the variation of phase angle with frequency at increasing nano graphite loadings. From the figure it can be observed that irrespective of amount of filler in the composite, at low frequencies the value of phase angle is close to 0^0 which corresponds to resistive characteristics [$Z \approx R$]. But with increase in frequency there is an increase in phase angle and reaches a peak in the range of 100 Hz at low filler loadings and at 10^4 Hz at high loadings of filler (2.5 and 3.5 phr). It can also be observed that as filler loading increases the maximum phase angle reaches about -80^0 which corresponds to capacitors [$Z \approx 1/j(2\pi fC)$].

Dielectric loss tangent

Figure 3 shows the variation in dielectric loss tangent as a variation of filler loadings and frequency. From the Figure it can be observed irrespective of filler loading there is a gradual decrease in loss

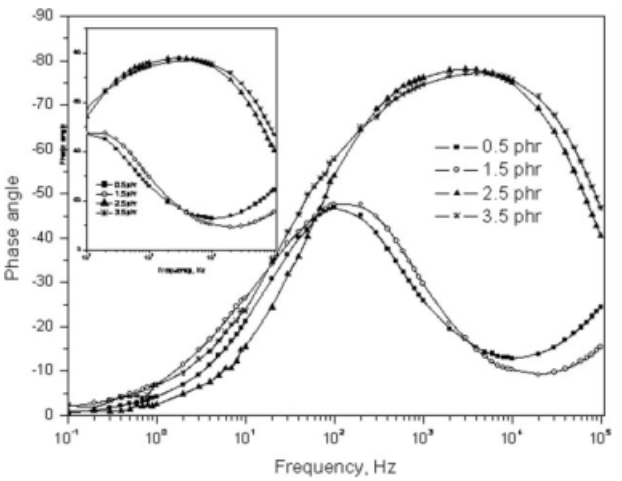

Figure 2 Variation in phase angle with increasing filler loadings and at increasing frequencies in flouroelastomer-expanded graphite nanocomposites.

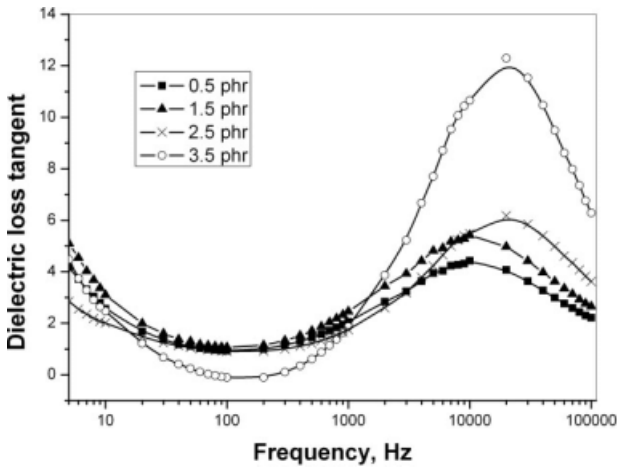

Figure 3 Variation in dielectric loss tangent with frequency at increasing graphite loadings in flouroelastomer-expanded graphite nanocomposites.

tangent values with increasing frequencies. But this increase is not continuous and at after reaching a maximum the loss tangent curve shows a decrease. The frequency at which this maximum is appearing depends on the nano graphite concentration and a maximum has been observed at 10263, 10531, 19385, and 20455 Hz at 0.5, 1.5, 2.5, and 3.5 phr, respectively. This increase in frequency can be explained on the basis of the mechanical and viscoelastic properties of crosslinked and reinforced multiphase polymeric materials. The addition of the filler particles has a significant effect on the dielectric behavior of the sample. Filler particles in the matrix acquires induction charges in presence of the applied external field, polarization effects take place the so called Maxwell-Wagner-Sillar's polarizations. Below the critical concentration of the filler loading, the interparticle distance is large enough so that neighboring local fields apparently do not interact. Thus dielectric factor in this region increases slowly. But as the filler loading increases, the Maxwell-Wagner-Sillar's

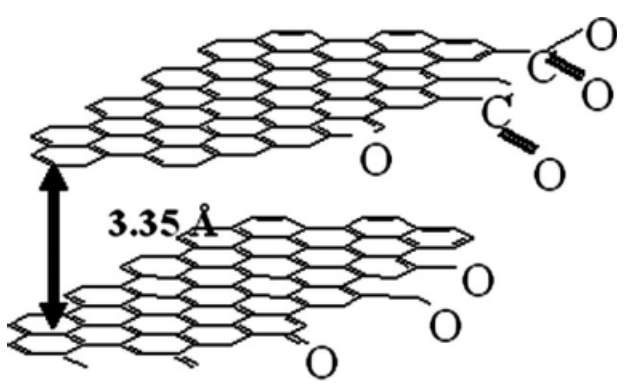

Figure 4 Schematic representation of the distribution of oxygen groups on the surface of graphite.

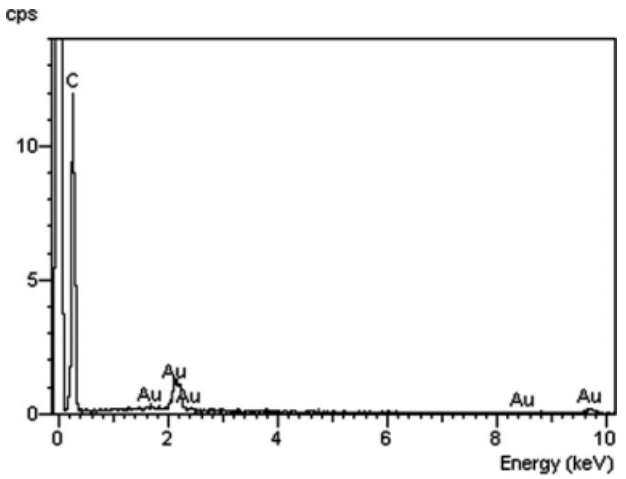

Figure 5 EDS spectra of graphite powder.

effect increases due to reduction in the interaggregate distance giving rise to dielectric properties.

Addition of functional fillers results in not only hydrodynamic interactions but also leads to complex physicochemical interactions between the polymer matrix and the filler surface.[11,12] These elastomer-filler interactions are often characterized by the content of the apparent "bound" rubber, which is determined as the amount of insoluble rubber adhering to the dispersed filler before vulcanization. Since the amount of bound rubber is related to the filler loading it can be regarded as a measure of the interactions between the filler and matrix.[13] Since the graphite used in the present study is acid treated, it has some oxygen functionality and a schematic representation of the same is shown in the Figure 4. The presence of oxygen in the exfoliated graphite powder has been tested by Electron dispersive spectra (EDS) and representative spectra of ordinary graphite and exfoliated graphite are shown in Figures 5 and 6, respectively. The elemental analysis of

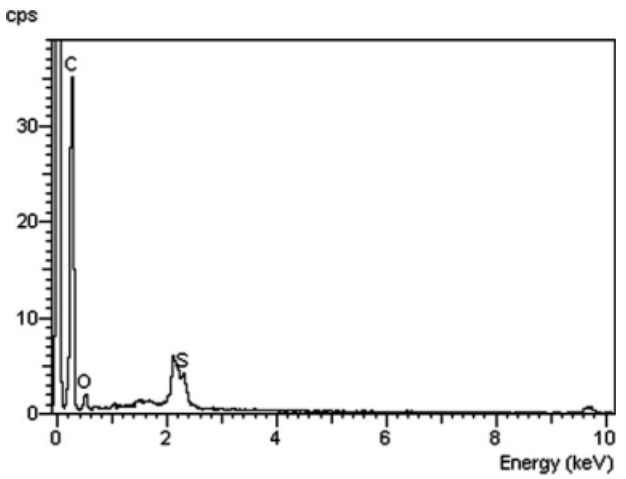

Figure 6 EDS spectra of nano-graphite powder.

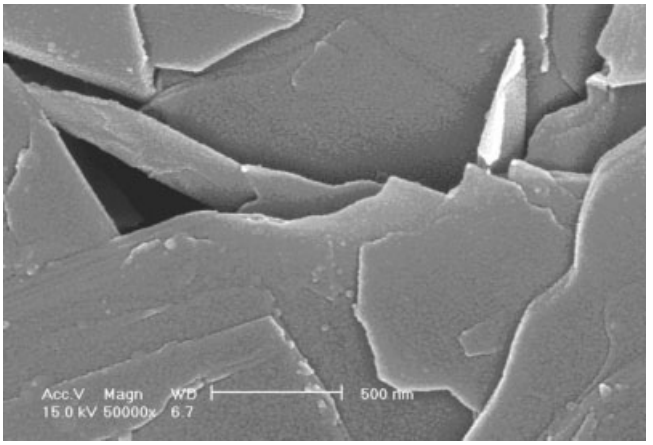

Figure 7 High resolution SEM microphotograph of exfoliated nano graphite sheets.

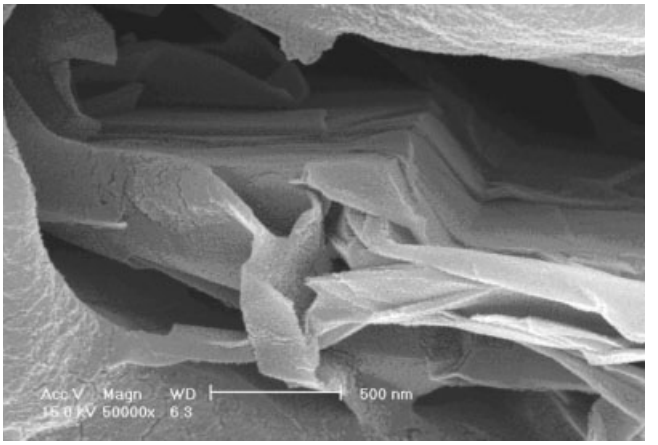

Figure 8 High resolution SEM microphotograph of nano graphite sheets extracted from the polymer compound after solvent (MEK) extraction.

exfoliated graphite show 85.09% carbon, 14.04% oxygen, and 0.87% sulfur. The presence of this oxygen increases the polymer filler interactions due the formation of complex physicochemical bonds between the filler surface and the polymer matrix. Increased filler loading leads to increase in polymer-filler interactions thereby making a portion of the polymer matrix attached to the filler surface. An SEM microphotograph of raw graphite powder and solvent (Methyl Ethyl Ketone) extracted graphite from the polymer compound taken at same length scales is shown in Figures 7 and 8, respectively.

From the figure it can be observed that the surface of graphite sheets in solvent extracted sample is rougher with increasing surface instabilities when compared with raw graphite sheets which indicate the adhesion of polymer chains onto the nanographitic layers. A more comprehensive study regarding reinforcement, mechanical, dynamic mechanical and fracture properties are published in our other manuscript.[14]

Impedance analysis

Figure 9 shows the variation of the imaginary component of the complex impedance (Z'') with frequency as a function of increasing filler loading in exfoliated nano graphite reinforced flouroelastomer vulcanizates. From the Figure it can be observed that with increase in frequency there is a gradual increase in complex impedance for all the vulcanizates reaching a maximum in the region of 10 Hz at low filler loadings (0.5 and 1.5 phr) and around 100 Hz at higher loadings (2.5 and 3.5 phr). This can be attributed to the secondary relaxation of the polymer chains of the flouroelastomer matrix. However, the observation of this additional peak in the imaginary component of impedance can also be attributed to the relaxation of the interfacial region between the polymer and the filler. Numerous examples of additional damping peaks have been cited[15–17] in the field of particulate reinforced polymeric systems. This can be explained on the basis of the mechanical and viscoelastic properties of crosslinked and reinforced multiphase polymeric materials. Generally polymer composites are crosslinked multiphase materials, the relaxation of which depends on molecular relaxation processes and morphology. Although these relaxations can usually be associated with each component, their appearance depends on the chemical and physical interactions of the two phases (filler and the polymer matrix). The filler used in this study (exfoliated nano graphite and prepared by acid intercalation technique), due to its high surface activity and the presence of oxygen shows good interaction with the polymer matrix, thereby leading to the formation of a strong interphase. The thickness of this interphase is inversely proportional to

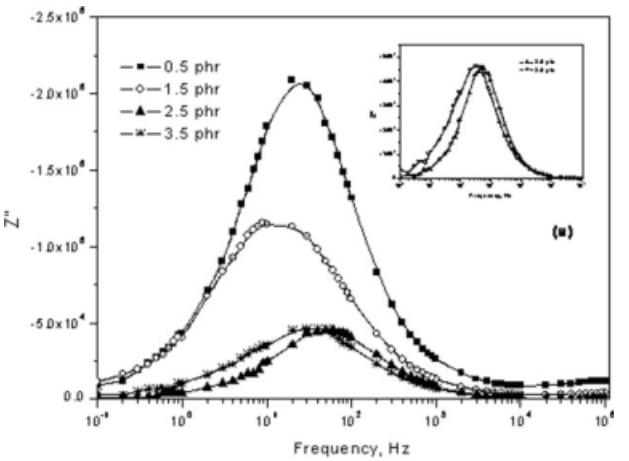

Figure 9 Variation in complex part of impedance with frequency at increasing graphite loadings in flouroelastomer-expanded graphite nanocomposites.

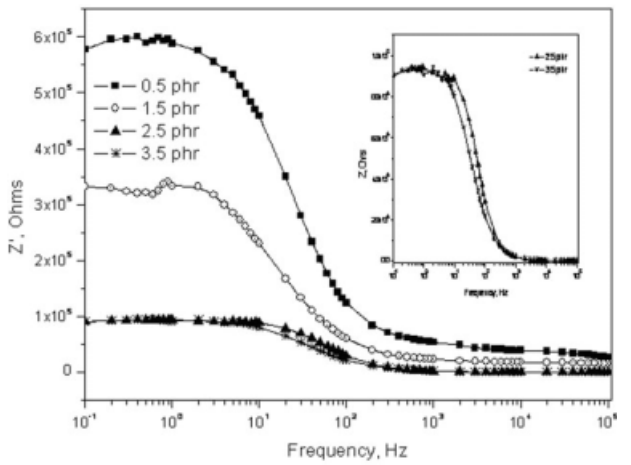

Figure 10 Variation in real part of impedance with frequency at increasing graphite loadings in flouroelastomer-expanded graphite nanocomposites.

the interfacial tension between the polymeric phases. Although the concept of an interphase has widely been recognized, its *in situ* detection and characterization is difficult. The properties of such an interfacial region differ from those of the pure components, and strongly affect the overall properties of the resulting material. As a consequence, an interphase can be considered to have a certain volume with its own characteristic properties or property gradients. A substantial portion of the polymer chains are expected to be in immobilized on the filler surface thus leading to the formation of regions of spatial heterogeneities. A polymer layer having a higher stiffness than the bulk polymer in the vicinity of the dispersed phase surface is created from restricted molecular mobility due to interactions between phases.[18] So, as the filler loading increases more and more polymer is adsorbed on the filler surface thereby making its relaxation difficult.

From the Figure it can also be observed that with increase in filler loading there is a gradual shift of frequency, but the intensity of this shift is more pronounced at lower filler loadings than at higher filler loadings which can be attributed to the occurrence of percolation phenomenon. (A detailed discussion about percolation is given in subsequent section).

A similar explanation can be extended to explain the variation in real part of impedance with frequency. Figure 10 shows the variation in real part of impedance (Z') versus frequency as a function of increasing concentration of nano graphite. With increase in frequency, there is a gradual reduction of the real part of impedance but only until the region of 1–100 Hz, beyond which Z' remains almost same for all the vulcanizates. This trend of continuous drop of impedance with applied frequency is a characteristic of a pure capacitor.

The Z'' data has been fitted to different spectral functions commonly used such as Debye, Cole-Cole, Cole-Davidson, Havriliak-Negami, Frohlich.[19] The best fit was obtained using a Havriliak-Negami function, superimposed with Frohlic function to account the effect of conductivity.

The spectral function $Z''(\omega)$ can be expressed as:

$$Z''(\omega) = Z''(\omega)_{HN} + Z''(\omega)_{Fr} + \frac{\theta\sigma}{\omega} \tag{2}$$

where $Z''(\omega)_{HN}$ denotes Havriliak-Negami function form and $Z''(\omega)_{Fr}$ denotes Frohlic function, ω denotes the angular frequency, σ is the DC conductivity and θ is a constant. Havriliak-Negami function is expressed as

$$Z''(\omega)_{HN} = \frac{(Z''_s - Z''_\infty)\sin\phi\beta}{\left[1 + 2(\omega\tau_{HN})^{1-\alpha}\sin\frac{\pi\alpha}{2} +)\omega\tau_{HN})^{2(1-\alpha)}\right]^{\beta/2}} \tag{3}$$

where

$$\phi = \arctan\frac{(\omega\tau_{HN})^{(1-\alpha)}\cos\frac{\pi\alpha}{2}}{1 + (\omega\tau_{HN})^{(1-\alpha)}\sin\frac{\pi\alpha}{2}} \tag{4}$$

and Z''_s and Z''_∞ are the values of Z''_s at static (at 0.01 Hz in our case) and at infinite frequency (10^5 Hz), respectively. The parameters α and β in have been found to be 0.186 and 0.587, respectively.

Frohlich function is represented as

$$Z''(\omega)_{Fr} = \frac{(Z''_s - Z''_\infty)}{P}\arctan\frac{\sinh P/2}{\cosh\ \ln(\omega\tau_{Fr})} \tag{5}$$

where P is a parameter describing the width of the distribution of relaxation times between the two limiting values τ_1 and τ_2 (where $P = \ln(\tau_1/\tau_2)$). τ_{Fr} is the mean relaxation time and is equal to $(\tau_1\tau_2)^{1/2}$. The values of τ_1 calculated at increasing nano graphite loadings of 0.5, 1.5, 2.5, and 3.5 phr is found to be in the range of 1.247×10^3, 2.547×10^3, 4.387×10^3, and 5.327×10^3 s, and τ_2 values as 3.324×10^4, 4.987×10^4, 5.698×10^4, and 7.012×10^4 s, respectively.

Nyquist plots

Figure 11 shows the Nyquist plot (the relationship between imaginary part of impedance (Z'') and real part of impedance (Z')) of fluoroelastomer vulcanizates as a function of filler loading. It can be observed that increasing filler in the composite has a sizable effect on the dielectric properties of this system at all frequencies. From the Figure it can also be observed that irrespective of the filler loadings, the plots yield good semicircles indicating the occurrence of polarization with a single relaxation time taking place, i.e., a local mode process dominated.

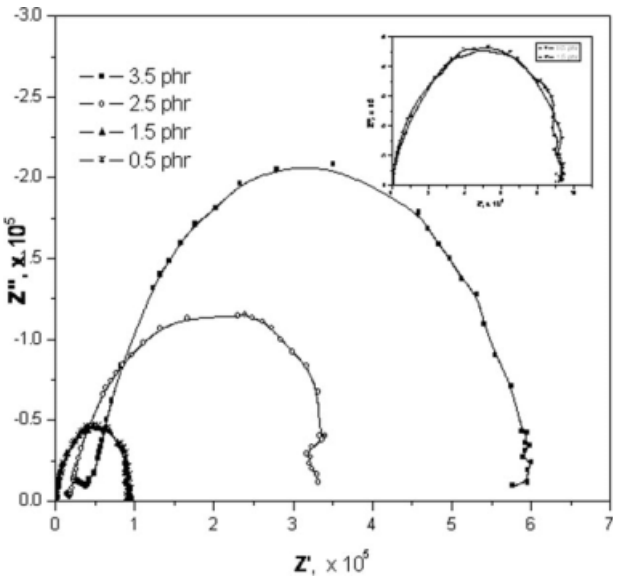

Figure 11 Nyquist plot of at increasing filler (nano graphite) loadings in flouroelastomer vulcanizates.

However, at higher filler loadings (2.5 and 3.5 phr), the semicircles did not reach the origin and had a small positive intercept on the Z' axis indicating build up of ions at the interphase between the filler and polymer matrix.[20,21]

Several attempts have been made to interpret the impedance spectroscopy of polymer-filler systems using the resistance-capacitance parallel circuit (R-C) model. Representative R-C Circuit model at low and high filler loadings is shown in Figure 12(a,b). According to this model[22] the overall impedance of a parallel circuit, (equal to the reciprocal overall admittance, Y^*), i.e., the sum of the contributions from resistance and capacitance and given by the equation

$$Z^* = \frac{1}{Y^*} = R_1 + \frac{1}{i\omega C_1} \tag{6}$$

where $i = (-1)^{1/2}$, ω is the angular frequency, $\omega = 2\pi f$, f is frequency and Z^* is the complex impedance, which consists of both real and imaginary parts. Here R_1 is the resistance of the circuit and C_1 is the capacitance.

In a Nyquist plot for a polymer composite system the real axis represents bulk resistivity (R_B) and the imaginary axis represents the ω_{max}, which is given by

$$\omega_{max} = \frac{1}{R_B C_B} \tag{7}$$

where C_B is the bulk capacitance of the polymer composite. In a Nyquist plot, increase in R_B represents poor conductivity. Figure 11 shows that with increase in filler loading, R_B decreases or in other words the conductivity of the composite increases.

With increasing filler loading the distance between the aggregates reduces. This gap can be approximated by a parallel plate capacitor with an area (A), separation distance (d), and capacitance (C) ($\varepsilon_0 A/d$), where ε is the dielectric constant of the polymer. Each filler aggregate has a resistance (Ra), the resistance within the aggregate. The impedance in a microcellular composite can be written as

$$Z = R_{as} + \frac{R_{cs}}{1 + \omega^2 R_{cs}^2 C_s^2} - j\frac{\omega R_{cs}^2 C_s}{1 + \omega^2 R_{cs}^2 C_s^2} \tag{8}$$

The respective imaginary and real parts of impedance can be expresses as

$$Z' = R_{as} + \frac{R_{cs}}{1 + \omega^2 R_{cs}^2 C_s^2} \quad \text{and} \quad Z'' = -\frac{\omega R_{cs}^2 C_s}{1 + \omega^2 R_{cs}^2 C_s^2} \tag{9}$$

and the dielectric loss tangent can be expressed as

$$\tan\,\partial = \frac{Z''}{Z'} = -\frac{\omega R_{cs}^2 C_s}{R_{as} + R_{cs} + \omega^2 R_{cs}^2 R_{as} C_s^2} \tag{10}$$

From above equations the relationship between Z' and Z'' is

$$\left(Z' - \frac{2R_{as} + R_{cs}}{2}\right)^2 + Z_2^2 = \left(\frac{R_{cs}}{2}\right)^2 \tag{11}$$

Therefore a plot of Z'' and Z' will give a half circle which has the center at $((2R_{as} + R_{cs})/2,0)$ and radius of $R'_{cs}/2$.

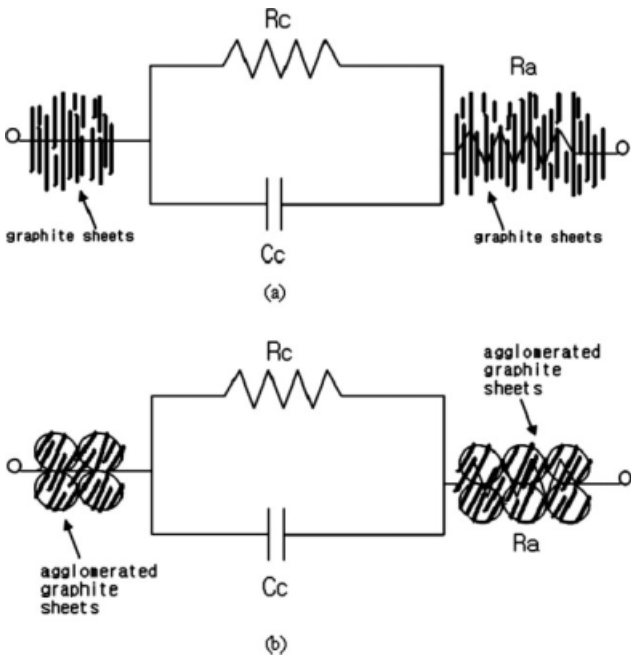

Figure 12 R-C circuit representation of nano graphite reinforced flouroelastomers at low (a) and high loadings (b).

TABLE I
Radius and Center (for Fig. 11) in Nano Graphite Reinforced Fluoroelastomer Vulcanizates

Filler loading (phr)	Center (x, 0)	Radius
0.5	3.424×10^5, 0	1.98×10^5
1.5	2.273×10^5, 0	0.87×10^5
2.5	4.358×10^4, 0	4.42×10^4
3.5	4.462×10^4, 0	4.34×10^4

Wang et al.[23] proposed that since the circular curve of the Z″ versus Z′ occurs only for the parallel resistor circuit, the above analysis can be used to confirm the existence of the capacitor effect. The capacitor effect also confirms that the gaps between the filler aggregates controls the electron conduction via non-Ohmic contacts between the filler aggregates. The variation in the values of radius and center of the half circle can also be used as a measure of the gaps in between filler aggregates. Using the above equations, the radius and center has been calculated and tabulated in Table I. It can be observed that increasing filler loadings the radius reduces and the center shifts to lower values.

It can also be observed that with increasing nano graphite loadings the area under the curve in the Nyquist plot is decreasing. The intensity of this decrease is more pronounced at higher loadings of filler when compared with lower loadings. This can be explained on the basis of "space charge" phenomenon in heterogeneous systems. Filled rubbers are multicomponent systems that have complex molecular, supramolecular and topological structures, which determine their ultimate properties. These structures are formed during compounding and processing.

The sample preparation of rubber involves operations such as compression, cutting and friction, which cause electrical polarization that leads to the formation of the so called mechano-electrets.[24] The lifetime of the polarization charge depends on the polymer nature and the conditions of electret storage and usage (temperature, dielectric characteristics of the polymer, fillers etc.) This electret state of rubbers has been studied in detail (especially the arising of the electret state during processing) by Pinchuk et al.[25] who proposed that nonconductive rubber when subjected to high shear stresses could lead to electret formation. These radicals could participate in polarization following several mechanisms: dipolar (directed orientation of molecules), ionic (orientation of quasi-dipoles created by weakly bonded ions) and bulk (radicals displacement to macrodistance). Increasing filler loadings lead to increased formation of more electrets thereby giving rise to more polarization.

A similar explanation has been given by Levya et al. who reported that the medium frequency relaxation in carbon black reinforced polymers is caused primarily by interfacial polarization, which is due to the build-up of charges on boundaries/interfaces between materials.[26] Application of an external electric field causes polarization of large colloidal particles, and creates perturbation in a miniature double layer on each particle, which behaves like a macroion.[27] Under the influence of an external electric field, the counter-ions are redistributed along the surface of filler particles, and hence a double layer is deformed and polarized, leading to interfacial polarization and the resulting relaxation or dispersion. The magnitude of relaxation of these counter-ions (in the medium frequency region) is much larger than the relaxation due to orientation of dipoles.[28]

Electric modulus

The electric modulus formalism has been used to further investigate the conductivity and relaxation phenomena in nano graphite reinforced flouroelastomers. The 'electric modulus' formalism, first introduced by McCrum et al.[29] and extensively used for the investigation of electrical relaxation phenomena in polymer composites by Tsangaris and coworkers[30,31] can be defined as the inverse quantity of complex permittivity and is given by the following expression:

$$M^* = \frac{1}{\varepsilon^*} = \frac{\varepsilon'}{\varepsilon'^2 + \varepsilon''^2} + j\frac{\varepsilon''}{\varepsilon'^2 + \varepsilon''^2} = M' + jM'' \qquad (12)$$

where M^* is the complex electric modulus, M' is the real and M'' is the imaginary part of electric modulus, ε' and ε'' are the real and imaginary parts of permittivity.

M^* (ω) characterizes the dynamic aspects of the charge motion in conductors in terms of relaxation in an electric field.[32] The plot of variation in M' with increasing filler loadings is shown in Figure 13. From the Figure it can be observed that with increasing filler loadings there is increase in modulus values, but after attainment of a critical frequency the increase is exponential in nature. From the Figure it can also be observed that irrespective of the amount of filler in the composite, the value of M' is nearly zero at low frequencies indicating that the electrode polarization gives a negligible low contribution to M' and can be ignored when the permittivity data is expressed in this form.[33] After keeping a low value, M' increases steeply in the range of 10–100 Hz at low filler loadings (0.5 and 1.5 phr) and at slightly higher range of 100–1000 Hz at higher loadings (2.5 and 3.5 phr).

Figure 14 shows the variation of the imaginary part of the modulus as a function of frequency at increasing filler loadings. The low value of M'' in the

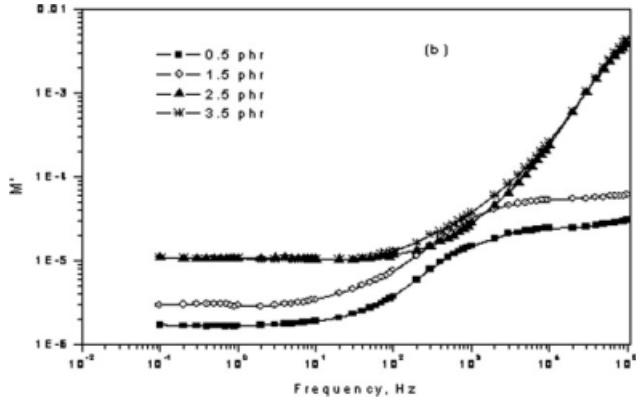

Figure 13 Variation in real part of electric modulus with frequency at increasing graphite loadings in flouroelastomer-expanded graphite nanocomposites.

low-frequency region suggests that electrode polarization makes negligible contribution to electric modulus at these frequencies. The broad nature of the M'' peaks can be interpreted as being the consequence of distributions of relaxation time. It can also be observed that with increase in filler loading, M'' peaks in general exhibit increasing peak heights and peak maximum shifts to higher frequencies. The M'' peaks are asymmetric and the widths are broader than ideal Debye peak thus indicating increasing Maxwell-Wagner-Sillar's polarization.

The variation of M'' with increasing frequencies also shows a nonmonomodal distribution of electric modulus. At low filler loadings, the value of M'' reaches a peak value in the range of 500 Hz at 0.5 phr and around 900 Hz in case of 1.5 phr loaded samples. Further increase in filler loadings is shifting the peak maximum to higher frequency region and could not be found due to instrumental limitations. But from the trends of the graphs indicate that with

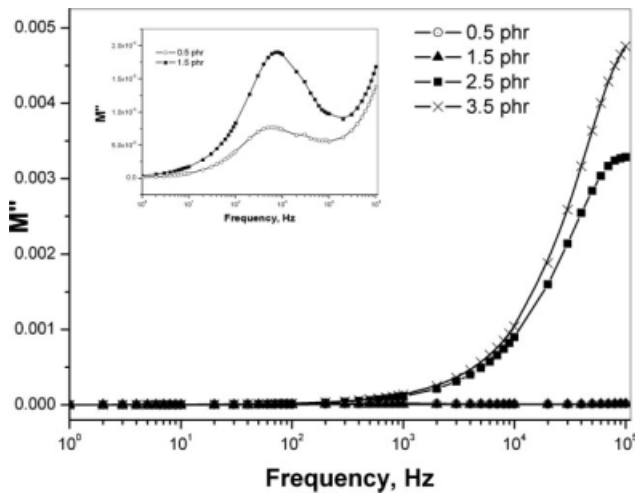

Figure 14 Variation in complex part of electric modulus with frequency at increasing graphite loadings in flouroelastomer-expanded graphite nanocomposites.

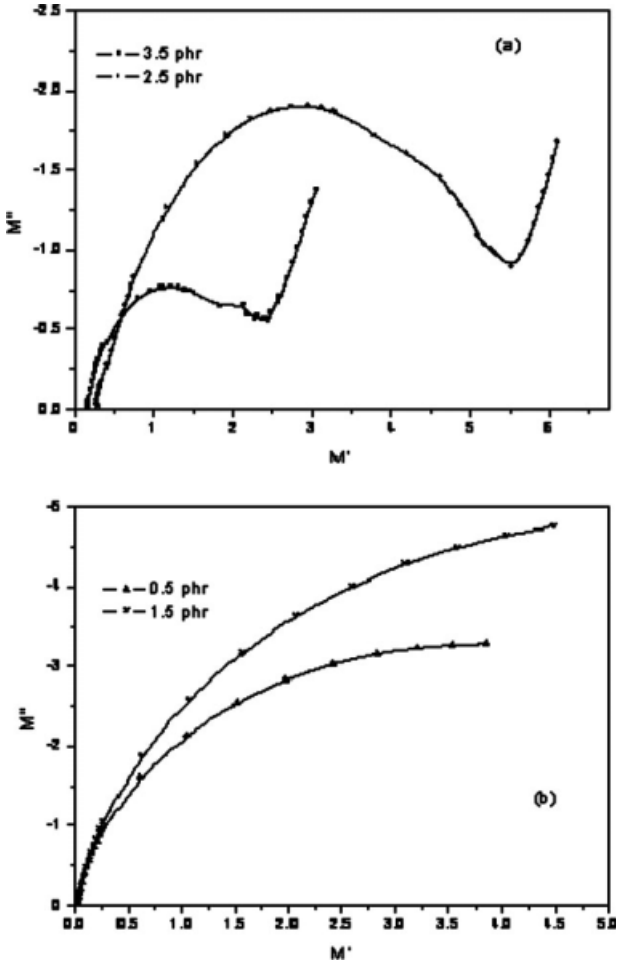

Figure 15 Cole-Cole plots of graphite-flouroelastomer nanocomposites.

increase in filler loading, the appearance of maximum value of M'' occurs at increasingly higher frequencies which is an indication of enhanced DC conductivity as predicted by theory and given by the expression

$$\sigma_{DC} = \frac{e_0}{M_\infty \langle \tau \rangle} \tag{13}$$

where M_∞ is the frequency at which the peak maximum occurs, $\langle \tau \rangle$ is the relaxation time calculated by the expression $\langle \tau \rangle = \frac{1}{2\pi f_{max}}$.

The Nyquist plots plotted as M'' vs. M' (Complex electric modulus versus electric modulus) at low and high loadings of fillers are shown in Figure 15(a,b). The advantage of M'' vs. M' is that it will offer better resolution than ε'' vs. ε' (Nyquist) plots (Complex impedance versus real impedance) when the difference between time constants is related to resistance, while the Nyquist plot is more capable of resolving time constants related to different capacitive values.[34] From the figures, it can be observed that at low filler loadings the shape of the curves are nearer to semicircle (after the experimentally obtained

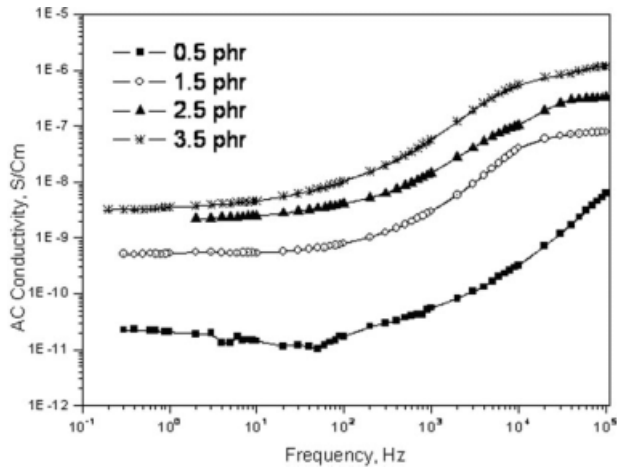

Figure 16 Variation in AC conductivity at increasing filler loadings and frequency in expanded graphite reinforced flouroelastomer nanocomposites.

curve is extrapolated to touch the X-axis), but at higher loadings of the filler, the semicircle becomes more skewed which can be explained on the basis of interfacial polarization. The inclusion of highly asymmetric particles in composites, such as nano graphite sheets, created an additional asymmetric distribution of relaxation times. It is then concluded that the inclusions intervene in the process of interfacial relaxation. A similar observation in Kevlar fiber reinforced Epoxy composites has been reported by Tsangaris et al.[30]

AC conductivity

Figure 16 shows the variation of electrical conductivity with frequency at different filler loadings in nano graphite reinforced flouroelastomer nanocomposites. It is widely believed that electrical properties of reinforced polymers depend primarily on the way the filler particles are distributed through the polymer matrix also called the mesostructure.[35] At low levels of filler loading the conductivity of the composite is slightly higher than that of the base polymer, since the filler particles are isolated from each other by the insulating polymer matrix. When the loading of filler is low, the conductivity between the grains of filler is expected to be primarily via hopping and tunneling mechanisms. In this mode of conduction, the electron transport may be coupled strongly with the molecular and ionic processes in the insulating polymer matrix. Usually, hopping transport between localized sites is the main reason for the frequency dependence of conductivity in polymer composites. The dispersion of filler is heterogeneous, localized and disordered. This disorder results in a wide distribution of hopping rates, giving a strong dispersion of the AC conductivity[36,37]

Considering the R-C parallel circuit model, with increase in filler loading, aggregation of the graphite sheets leads to more tight packing and more intensely pressed against each other. This leads to a net reduction in the internal contact resistance (R_C) and therefore, the net resistance ($R_C + R_A$) decreases with increase in the filler loading level. Here R_A and R_C indicates the inter and intraparticle aggregate resistance, respectively. The gaps between conducting particle agglomerates at high filler loading become very small or negligible and the net resistance becomes practically equal to R_A. This would usually happen for high enough loading using conducting filler. Hence conductivity increases with filler loading.[38]

Modeling of conductivity

According to Jonscher[39] the electrical conductivity of many disordered solids (including polymer composites) was found to be sum of DC conductivity (independent of frequency) and AC conductivity (strongly frequency dependent). It was noted that the overall frequency dependence of σ (so called 'universal dynamic response' of electron conductivity) could be approximated by the following simple relation:

$$\sigma = \sigma_{ac} + \sigma_{a.c.} \quad \text{or} \quad \sigma = \sigma_{ac} + A\omega^s \qquad (14)$$

where $\omega = 2\pi f$ is the angular frequency, A is constant and s are exponential parameter. For a polymer composite containing moderate concentration of filler, $s \approx 0.5$–0.6, and both s and A follow strong dependencies on a variety of factors including the filler loading and temperature. The values of A and s calculated for increasing nano graphite concentrations and is shown in Table II. From the Table, it can be observed that the value of both A and s increases on increasing volume fraction of filler, but the intensity of this increase is less at higher loadings of filler which indicates the occurrence of percolation due to the formation of continuous filler network.

Percolation

The variation of electrical conductivity with increasing filler loadings at various frequencies (10^2, 10^3,

TABLE II
Variation in *A* and *s* with Nano Graphite Loading in Reinforced Flouroelastomer Nanocomposites

Filler loading (phr)	*s*	*A*
0.5	0.113	32.356
1.5	0.276	41.987
2.5	0.342	53.843
3.5	0.461	62.981

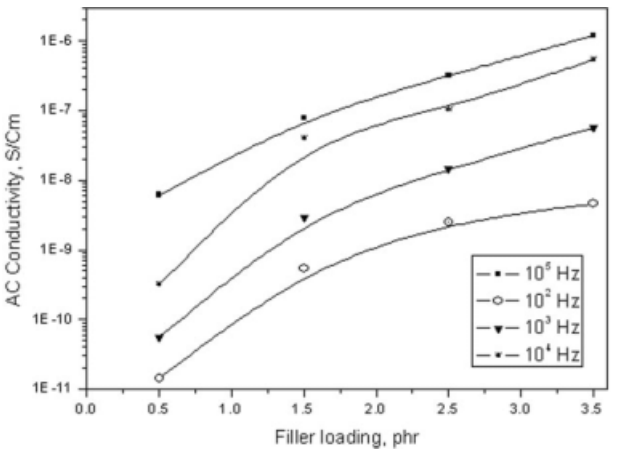

Figure 17 Effect of filler loading on conductivity at various frequencies.

10^4, and 10^5 Hz) is shown in Figure 17. It can be observed that irrespective of the frequency all the samples show an abrupt increase in conductivity after 2.5 phr loading of filler. The electrical conductivity of a composite is generally characterized by its dependence on filler volume fraction. As the filler amount in the composite is increased, the filler particles begin to contact each other and a continuous path is formed through the volume of the sample for electrons to travel. The formation of this conductive network is based on the principles of percolation theory. The initiation of percolation theory is attributed to Hammersley and Broadbent in 1957.[40] Medalia in his review on electrical conduction in carbon black reinforced composites explained that percolation is due to tunneling of electrons and the conductivity is controlled by the gaps between the carbon black aggregates.[41] As the filler loading increases the nanographite sheets aggregate eventually forming agglomerates. The electrical conductance in these type of heterogeneous polymer composites depend on the distance between the aggregates, hence composites can be regarded as the system composed of random arrays of closely spaced conductors dispersed in an insulating polymer matrix. Experimental results for composites consisting of an insulating matrix and conductive filler particles are often analyzed in terms of statistical percolation theory. Beyond a critical concentration of the filler, known as the percolation threshold, an increase of the composite conductivity of several orders of magnitude is observed. The theoretical value of the percolation threshold for randomly-dispersed, hard, spherical particles has been determined to be about 16 vol %.[42] However, in epoxy composites, percolation thresholds of less than 1 vol % of spherical carbon black particles have also been reported.[43] Percolation limit of the nano graphite sheets in this study seems to occur between 2.5 and 3.5 phr loading. This is slightly above the percolation limit of nano graphite reinforced polypropylene composites reported by Drzal and coworkers.[9] This deviation can be attributed to the filler distribution and formation of mesostructure arising due to complex molecular scale forces and interactions. SEM microphotographs of 2.5 and 3.5 phr loaded flouroelastomer vulcanizates have been shown in Figure 18(a,b). From the figure agglomeration and aggregation of nano graphite platelets can be distinctly observed.

CONCLUSIONS

The dielectric relaxation of exfoliated nano graphite reinforced flouroelastomer vulcanizates has been studied as function of increasing filler loading and blowing agent loadings in the frequency range of 0.01–10^5 Hz. With increase in filler loading an increase in dielectric loss tangent has been observed which was explained on the basis of visco-elastic nature of the composites. Irrespective of the amount

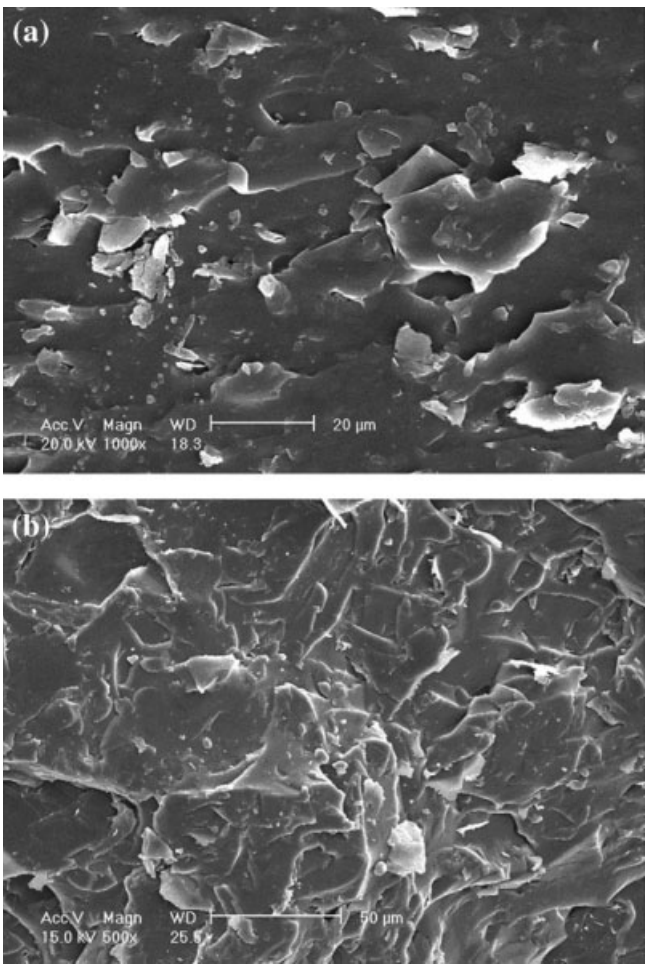

Figure 18 SEM microphotographs of 2.5 and 3.5 phr nano graphite reinforced flouroelastomer vulcanizates.

of filler in the composite a decrease in real part of impedance with increasing frequencies has been observed, which was indicative of the capacitance nature of the composites. The variation of complex part of impedance with applied frequency showed a distinct peak, the occurrence of which was dependent on the amount of filler in the composite. Increasing filler loadings also lead to increase in non semicircle nature of the Nyquist plots. This phenomenon was analyzed on the basis of resistance-capacitance circuit. The percolation limit of the filler in the composite has been studied by electrical conductivity measurements. It has been observed that the percolation limit was occurring in between 2.5 and 3.5 phr loading.

References

1. MacFarland, E. W.; Weinberg, W. H. TIBTECH 1999, 17, 107.
2. Gilomini, P.; Brechet, Y. Model Simulat Mater Sci Eng 1999, 7, 8054.
3. Psarras, G. C.; Manolakaki, E.; Tsangaris, G. M. Compos A Appl Sci Manuf 2002, 33, 375.
4. Das, N. C.; Khastagir, D.; Chaki, T. K. J Appl Polym Sci 2003, 90, 2073.
5. Brosseau, C.; Molinié, P.; Boulic, F.; Carmona, F. J Appl Phys 2001, 89, 8297.
6. Sridhar, V.; Chaudhary, R. N. P.; Tripathy, D. K. J Appl Polym Sci 2006, 100, 3161.
7. Katsuno, T.; Chen, X.; Yang, S.; Motojima, S.; Homma, M.; Maeno, T.; Konyo, M. Appl Phys Lett 2006, 88, 232115.
8. Chen, G.; Wu, C.; Weng, W.; Wu D.; Yan, W. Polymer 2003, 44, 1781.
9. Fukushima, H.; Drzal, L. T.; Rook, B. P.; Rich, M. J. J Therm Anal Calorim 2006, 85, 235.
10. Kalaitzidou, K.; Fukushima, H.; Drzal, L. T. Compos Sci Technol 2007, 67, 2045.
11. Huber, G.; Vilgis, T. A. Macromolecules 2002, 35, 9204.
12. Kluppel, M.; Heinrich, G. Rubber Chem Tech 1995, 68, 623.
13. Donnet, J. B.; Rigaut, M.; Frustenberger, R. Carbon 1973, 11, 153.
14. Deng Xu; Sridhar, V.; Thanh Tu Pham; Kim, J. K. e-Polymers, to appear.
15. Nielsen, L. E.; Lewis, T. B. J Polym Sci Polym Phys Ed 1969, 7, 1705.
16. Eklind, H.; Schantz, S.; Maurer, F. H. J.; Jannasch, P.; Wesslen, B. 1996, 29, 984.
17. Eklind, H.; Maurer, F. H. J.; Steeman, P.; A. M. Polymer 1997, 38, 1047.
18. Shalaby, S. W. Thermal Characterization of Polymeric Materials; Turi, E., Ed; Academic Press: London, 1981.
19. Mc-Crum, N. G.; Read, B. E.; Williams, G. Anelastic and Dielectric Effects in Polymeric Solids, Dover ed.; Dover Inc.: New York, 1991.
20. Day, D. R.; Lewis, T. J.; Lee, H. L.; Senturia, S. D. J Adhes 1985, 18, 73.
21. Jawad, S. A.; Alnajjar, A. Polym Int 1997, 44, 208.
22. Kremer, F.; Schönhals, A. Broadband Dielectric Spectroscopy; Springer: New York, 2001, p 354.
23. Wang, Y. J.; Pan, Y.; Zhang, X. W.; Tan, K. J Appl Polym Sci 2005, 98, 1344.
24. Kestelman, V.; Pinchuk, L.; Goldade, V. Electrets in Engineering: Fundamentals and Applications; Kluwer Academic Publishers: Boston, 2000, p 281.
25. Pinchuk, L.; Jurkowski, B.; Jurkowoska, B.; Kravtov, A.; Goldade, V. Eur Polym J 2001, 37, 2239.
26. Leyva, M. E.; Barra, G. M. O.; Moreira, A. C. F.; Soares, B. G.; Khastgir, D. J Polym Sci Part B Polym Phys 2003, 41, 2983.
27. Grimnes, S.; Martinsen, O. G. Bioimpedance and Bioelectricity Basics, 1st ed.; Academic Press: New York, 2000.
28. Bearchell, C. A.; Edgar, J. A.; Heyes, D. M.; Taylor, S. E. J Colloid Interface Sci 1999, 210, 231.
29. McCrum, N. G.; Read, B. E.; Williams, G.; Anelastic and Dielectric Effects in Polymeric Solids; Wiley: London, 1967, p. 108.
30. Tsangaris, G. M.; Psarras, G. C.; Kouloumbi, N. J Mater Sci 1998, 33, 2027.
31. Psarras, G. C.; Manolakaki, E.; Tsangaris, G.M. Compos A Appl Sci Manuf 2002, 33, 375.
32. Han, M. G.; Im, S. S. J Appl Polym Sci 2001, 82, 2760.
33. Lee, H. T.; Chuang, K. R.; Chen, S. A.; Wei, P. K.; Hsu, J. H.; Fann, W. Macromolecules 1995, 28, 7645.
34. Gon Han, D.; Man Choi, G. Electrochim Acta 1999, 44, 4155.
35. Pike, O. E.; Seager, C. H. J Appl Phys 1977, 48, 5152.
36. Ghosh, P.; Chakrabarti, A. Eur Polym J 2000, 36, 1043.
37. Bottger, H.; Bryskin, V. V. Hopping Conduction in Solids, Berlin: Akademie-Verlag, 1985.
38. Knite, M.; Teteris, V.; Kiploka, A.; Klemenoks, I. Adv Eng Mater 2004, 6, 742.
39. Jonscher, A. K. Nature 1979, 267, 673.
40. Broadbent, S. R.; Hammersley, J. M. Proc Camb Phil Soc 1957, 53, 629.
41. Medalia, A. I. Rubber Chem Technol 1986, 59, 432.
42. Kirkpatrick, S. Rev Mod Phys 1973, 45, 574.
43. Schculer, R.; Petermann, J.; Schulte, K.; Wentzel, H. P. Macromol Symp. 1996, 104, 261.